

---

# Template-Based and Template-Free Approaches in Cellular Cryo-Electron Tomography Structural Pattern Mining

Xindi Wu<sup>1</sup> • Xiangrui Zeng<sup>1</sup> • Zhenxi Zhu<sup>2</sup> • Xin Gao<sup>3</sup> • Min Xu<sup>1</sup>

<sup>1</sup>Computational Biology Department, Carnegie Mellon University, Pittsburgh, PA, USA;

<sup>2</sup>Beijing University of Posts and Telecommunications, Beijing, China; <sup>3</sup>King Abdullah University of Science and Technology (KAUST), Computational Bioscience Research Center (CBRC), Computer, Electrical and Mathematical Sciences and Engineering (CEMSE) Division, Thuwal, Saudi Arabia

**Author for correspondence:** Min Xu, Computational Biology Department, Carnegie Mellon University, Pittsburgh, 15213, PA, USA. Email: mxu1@cs.cmu.edu

Doi: <http://dx.doi.org/10.15586/computationalbiology.2019.ch11>

---

**Abstract:** Cryo-electron tomography (Cryo-ET) has made possible the observation of cellular organelles and macromolecular complexes at nanometer resolution in native conformations. Without disrupting the cell, Cryo-ET directly visualizes both known and unknown structures in situ and reveals their spatial and organizational relationships. Consequently, structural pattern mining (a.k.a. visual proteomics) needs to be performed to detect, identify and recover different sub-cellular components and their spatial organization in a systematic fashion for further biomedical analysis and interpretation. This chapter presents three major Cryo-ET structural pattern mining approaches to give an overview of traditional methods and recent advances in Cryo-ET data analysis. Template-based, supervised deep learning-based and template-free approaches are introduced in detail. Examples of recent biological and medical applications and future perspectives are provided.

**Keywords:** cryo-electron tomography; deep learning; macromolecular complexes; structural pattern mining; visual proteomics

---

In: *Computational Biology*. Holger Husi (Editor), Codon Publications, Brisbane, Australia. ISBN: 978-0-9944381-9-5; Doi: <http://dx.doi.org/10.15586/computationalbiology.2019>

**Copyright:** The Authors.

**License:** This open access article is licensed under Creative Commons Attribution 4.0 International (CC BY 4.0). <https://creativecommons.org/licenses/by-nc/4.0/>

## INTRODUCTION

Cryo-electron tomography (Cryo-ET) is a powerful diagnostic and research tool that combines specimen cryo-fixation and multi-angle electron microscopy imaging (1), which enables structural biologists to produce three-dimensional (3D) volume reconstructions of near-native state cells and determine the structure of sub-cellular structures with molecular-scale resolution (2). Those images contain information about the 3D cell structure projected into a single plane. In order to recover the actual 3D arrangement of components in the specimen, the information in 2D projection images should be integrated computationally. Cryo-EM has experienced a dramatic increase in the attainable resolution of 3D reconstructions. Complexes with high intrinsic contrast, such as ribosomes, have been successfully analyzed. The discrete conformation of membrane receptors can be recognized, which provides a theoretical basis for exploring the structural basis of signals in the whole cell.

In recent years, the amount of information about molecular roles involved in cellular processes has increased dramatically, and it has become possible to detect or obtain cellular tomograms with information about macromolecular complexes, their structures and spatial positions in the cell. Proteomics, based on genomics and mass spectrometry, has carried out a comprehensive analysis of the cell proteome. Nevertheless, it is still very challenging to discover the structure of unknown complexes in tomograms. Due to various shapes, sizes, cellular abundance of unlabeled complexes, high crowding levels, limitations of template libraries, low signal-to-noise ratio (SNR) and the limited range of tilt angles (3), the structural discovery can be detected by structure pattern mining methods. The methods for molecular separation and purification for structural and functional studies have been a great success. This chapter focuses on three major Cryo-ET structural pattern mining approaches, giving an overview of traditional methods and recent advances in Cryo-ET data analysis. Template-based, supervised deep learning-based and template-free approaches are included. Examples of recent applications in biology and medical field along with future perspectives are discussed.

---

## TEMPLATE-BASED STRUCTURAL PATTERN MINING

Template search/match has been the most popular template-based method for detecting spatial location and orientation of a known structure of interest. The visual proteomics method is capable of identifying individual protein complexes in intact cells (4). A guide on how to implement the visual proteomics method was proposed by Förster and colleagues (5). There are three main processing steps included in this method. First, a library containing the reference structure of the target protein complexes resampled to the relevant electron optical conditions is assembled. Second, for all possible positions and directions, the local cross-correlation coefficient between each reference structure and tomogram is calculated and stored in the cross-correlation volume. Finally, the distribution of

cross-correlation values in these volumes is translated into a list of locations by peak extraction and statistical methods. For data acquisition, an experimental setup is required. It is desirable to obtain the highest quality frozen electron tomography in terms of SNR, and the dosage spent on the specimen during the acquisition should be well controlled. Recommendations on choosing acquisition parameters after analyzing the different factors on signal content in Cryo-ET can be found in this work (5).

The template-matching process includes four parts: handling MolMatch, creating motif lists, scoring and visualization of molecular atlases. The scoring function (SF) for visual proteomics (6) relies on three different knowledge-based, empirical readouts. Besides, they also discuss other technical improvements. To detect low-abundance protein complexes with confidence, data acquisition and post-processing should be paid enough attention. The signal in visual proteomics is due to the contrast given by the surrounding solvent, so a better dosage control during the data acquisition is unavoidable. Also, phase plates may help to obtain a better performance. The electron dose that can be applied to the specimen limits the resolution that can be achieved by Cryo-ET, which leads to the limitation of the Cryo-ET application in visual proteomics.

It is important to assess whether the subtomogram, which is a small 3D cubic subvolume containing one macromolecular complex, or the recovered structure can be matched to a particular known structure. A template-match calculates the structural correlation between a subtomogram or a recovered structure with a known structural template. However, a simple correlation score cannot fully conclude the template matching. Rigorous statistical tests need to be carried out. Wang et al. (7) proposed a Monte Carlo sampling hypothesis testing framework based on generative adversarial network modeling for assessing template matching results. First, a generative adversarial network is constructed by using known structures to generate the structural distribution of macromolecular complexes. The structural generator is trained to the extent that the discriminator cannot distinguish between a known structure and a pseudo one. Second, a large number of pseudo macromolecular complexes are generated from the learned structural distribution in a Monte Carlo sampling fashion. Third, the subtomogram or recovered structure of interest is compared to the known structure and pseudo structure to assess the statistical confidence of template matching. This method computes not only a correlation score of template matching but also the P-value of whether the structure is significantly close to the template. Such a statistical assessment provides rigorous evidence of template matching and reduces its false-positive rate.

---

## **SUPERVISED SUBTOMOGRAM CLASSIFICATION AND SEGMENTATION**

Since 2017, supervised deep learning approaches, including classification and semantic segmentation, have been applied to Cryo-ET.

## Semantic segmentation using convolutional neural networks

The first deep learning-based semantic segmentation framework proposed for Cryo-ET data (8) classifies tomogram 2D slices in a voxel-wise binary fashion. With training data voxel-labeled manually, it predicts the segmentation mask of ribosomes, mitochondrial membrane, microtubules, and vesicles. To facilitate the prediction of membrane structures in different orientations, data augmentation was integrated into the training process with a moderately increased computational cost.

3D ConvNet (9) is a 3D semantic segmentation model for Cryo-ET data based on the U-Net architecture. 3D ConvNet predicts the segmentation mask of ribosomes, membrane and membrane-bound ribosomes in a multi-class fashion. As a result, the computational time does not increase linearly with the increase of class numbers (8).

Two 3D semantic segmentation convolutional neural networks (SSN3D) and their variants segmenting the main structural region from subtomograms have been proposed (10). This is a very useful step in subtomogram analysis because masking out neighboring structures can significantly reduce the structural bias for further analysis such as averaging and classification. Inspired by encoder-decoder type segmentation networks and fully connected networks, the networks are designed to be an encoder connected to a decoder inputting both high-level features and low-level features. The encoder is designed with alternation of convolution layers and max-pooling layers. The decoder is designed with alternation and convolution layers and upsampling layers. By combining different types of layers and combining both high-level and low-level feature information, the two segmentation networks can achieve high accuracy in 3D subtomogram semantic segmentation tasks.

## Subtomogram classification

Similarly, a deep learning-based particle subdivision approach (11) proposes two convolutional neural networks, namely Inception3D network and DSRF3D network, for subdividing heterogeneous subtomograms into some homogeneous subsets. After extracting features from subtomograms using the Inception3D or DSRF3D network, unsupervised clustering can be applied. Furthermore, it was demonstrated that the generalization ability of models of novel structures that do not exist in the training data can still be discovered and clustered. Based on this work, Che et al. (12) proposed three convolutional neural networks with promising classification performance for datasets of extremely low SNR (0.01): (i) DSRF3Dv2, an extended version of DSRF3D (Deep Small Receptive Field 3D); (ii) RB3D, a 3D residual block-based neural network; and (iii) CB3D, a convolutional 3D (C3D)-based model, with improved classification accuracy. Among these, the CB3D achieves the best performances and yields accuracy close to 0.9 for normal datasets.

## Model compression

Guo et al. (13) proposed a model compression approach for Cryo-ET data. Based on the deep neural network employed for the classification of

subtomograms, knowledge distillation to compress such networks was used. In previous works related to model compression on 2D images (14, 15), a model compression approach through knowledge distillation was proposed in order to speed up the separation of macromolecules at the prediction stage. The DSRF3D-v2 (Deep Small Receptive Field) model was chosen for compression considering the processing time and performance among the pre-existing models (12). Three student networks have been proposed to reduce the number of layers and parameters. The student network is a simplification of the teacher network. The compression includes compressing convolutional layers, pooling layers and eliminating one of the two fully connected layers. Reduction of the number of filters leads to simpler convolutional layers. DSRF3D-v2-s1 achieved the best performance by increasing the pooling size and stride from  $2 \times 2 \times 2$  to  $3 \times 3 \times 3$  and dismissing the dropout layers and one fully connected layer. Usually, a higher compression rate will lead to a greater loss of accuracy. Distilled models proposed in this study reduce the number of parameters, time and cost, and improve accuracy.

## Domain adaptation

For Cryo-ET, it is usually time-consuming and computationally intensive to create valid training data due to a massive demand for labeled training data. Obtaining training data from a separate data source where the annotations are readily available or can be executed in a high-throughput manner would be beneficial. The challenge is that the cross-data source prediction is often biased due to the different image-intensity distributions (a.k.a. domain shift). Domain adaptation has been shown to be beneficial for addressing this challenge. Lin et al. (16) adopted an adversarial domain adaptation framework called 3D-ADA for the structural classification of macromolecules captured by Cryo-ET. In order to obtain a robust model for a cross-data source macromolecular structural classification, this framework utilizes 3D convolutional neural networks and adversarial learning, mapping subtomograms into a latent space shareable between separate domains. Also, the training-feature extractions on multiple source domains can extend 3D-ADA to utilize multiple training data sources of Cryo-ET. Covariate shift is a typical case of domain shift (17). Compared to the original adversarial domain adaptation method (18), they have several modifications: (i) 2D CNNs to 3D with new 3D network architectures for Cryo-ET; (ii) two independent feature extractors to extract features from both source and target domains, making target domain features more robust; (iii) independent feature extractor for target data to enable the target domain feature to be more flexible and robust; and (iv) gradient forwarding of adversarial loss function. To avoid a local minimum for the model, the adversarial loss uses the proper domain supervision information for both the adversarial discriminator and the feature extractor training that avoids gradient vanishing in back-propagation.

## Simultaneous classification and segmentation by multi-task learning

Built on the above semantic segmentation and classification model, a multi-task learning neural network model was proposed (19) to perform semantic

segmentation, classification and coarse structural recovery (regression) simultaneously. The feature extraction layers are shared, which later split into three networks to perform each individual task independently; the loss of each task is linearly combined. This network design allows the training of the three tasks to mutually reinforce each other for better feature extraction and therefore higher accuracy. The accuracy of this model for classification and semantic segmentation outperformed single-task models (10, 11).

---

## TEMPLATE-FREE STRUCTURAL PATTERN MINING

Template-based methods have their own shortcomings due to the possibility that the template structure can misfit its targets. If the template structures come from different organisms, there will be different conformations in the template structures. Also, the conformational changes or additional bound components to the structure *in vivo* can be challenging to template-based methods. Under such circumstances, several template-free structural pattern mining methods have been proposed recently.

### De novo structural pattern mining via multi-pattern pursuit

A framework called multi-pattern pursuit (MPP) was designed for discovering frequently occurred structural patterns in Cryo-ET (3). It formulates the template-free visual proteomics analysis as a *de novo* pattern mining problem. The aim of MPP is to cluster, detect and estimate the abundance of large-scale complexes inside single cells automatically.

In this framework, first, after subtomograms are detected using template-free particle picking methods (20, 21), feature patterns are initialized. Second, initialized feature patterns are assessed for adding to the pattern library. Third, patterns are selected and aligned into common frames. Fourth, subtomograms are aligned with the candidate patterns and redundant patterns are discarded. The steps are iterated until high-quality patterns are distinguished and further refined individually. Therefore, representative and abundant patterns in a tomogram can be discovered without templates of known structures. Moreover, after patterns are successfully discovered, they can be embedded in the tomogram to visually present or statistically analyze their spatial distributions and interactions.

After the above subtomogram data processing steps, one of the most crucial steps is to average and cluster the subtomograms. To recover the structure of macromolecular complexes inside subtomograms which are heavily distorted by the noise and missing wedge effects, the use of a large number of subtomograms (usually more than a thousand) containing the same structure and averaging is recommended. The averaging process includes rotating and translating each subtomogram in a reference-free fashion because guidance from the known structures may bias the structural recovery. Only if the macromolecular complexes in the subtomograms are rotated and translated to a homogeneous orientation, and centered, the underlying true structure can be fully recovered

from averaging. The task becomes more challenging when there are multiple classes of subtomograms, meaning that different subtomograms may contain different macromolecular complexes. Averaging as well as clustering need to be refined during each iteration (22–24).

### Autoencoder for mining abundant and representative features

A convolutional autoencoder-based unsupervised approach has been proposed (25) for coarse selection of subtomograms of interest from a large number of subtomograms (scale ranging from thousands to millions). After subtomograms are extracted from the tomogram using particle picking methods, an optional pose normalization approach is provided to adjust the particle orientation and center for better clustering of the same structures of different orientations, which simplifies the process of structural mining. It also assists the image-features characterization in a less orientation-dependent way. A convolutional neural network is designed for encoding each subtomogram into a feature vector and decoding the feature vector to reconstruct the tomogram. K-means clustering algorithms and autoencoder networks are combined together to cluster Cryo-ET small-subvolumes into sets with homogeneous image features. Subtomogram-cluster centers are decoded and plotted for visual guidance for selection. Therefore, selecting among a large number of subtomograms becomes selecting among a few (usually less than a hundred) clusters. Interesting clusters, such as clusters of membrane features or globule features can be selected for further analysis. In addition, we designed a weakly supervised semantic segmentation convolutional neural network to which results from the convolutional autoencoder can be applied.

As illustrated in Figure 1, the autoencoder and MPP can be integrated into an unsupervised pipeline for template-free recovery of representative structures. Although the current template-free structural pattern mining approach is still more of proof-of-concept, when more and more unsupervised methods are developed in the future, we expect a powerful system of template-free methods to accurately and efficiently detect and recover both the known and unknown representative structures in a systematic fashion (26).

---

## CRYO-ET BIOLOGICAL AND MEDICAL APPLICATIONS

Due to the ability of Cryo-ET that can reveal the native structure and arrangement of macromolecular complexes inside intact cells, a lot of investigations have used this method to better understand the structural information of cells. Recently, there has been growing interest in establishing Cryo-ET as a diagnostic approach to complement conventional methods. Some recent examples of structural discovery and medical application using Cryo-ET are discussed in the following section. The increasing number of Cryo-ET medical applications demonstrates the potential of establishing Cryo-ET as a powerful diagnostic tool.

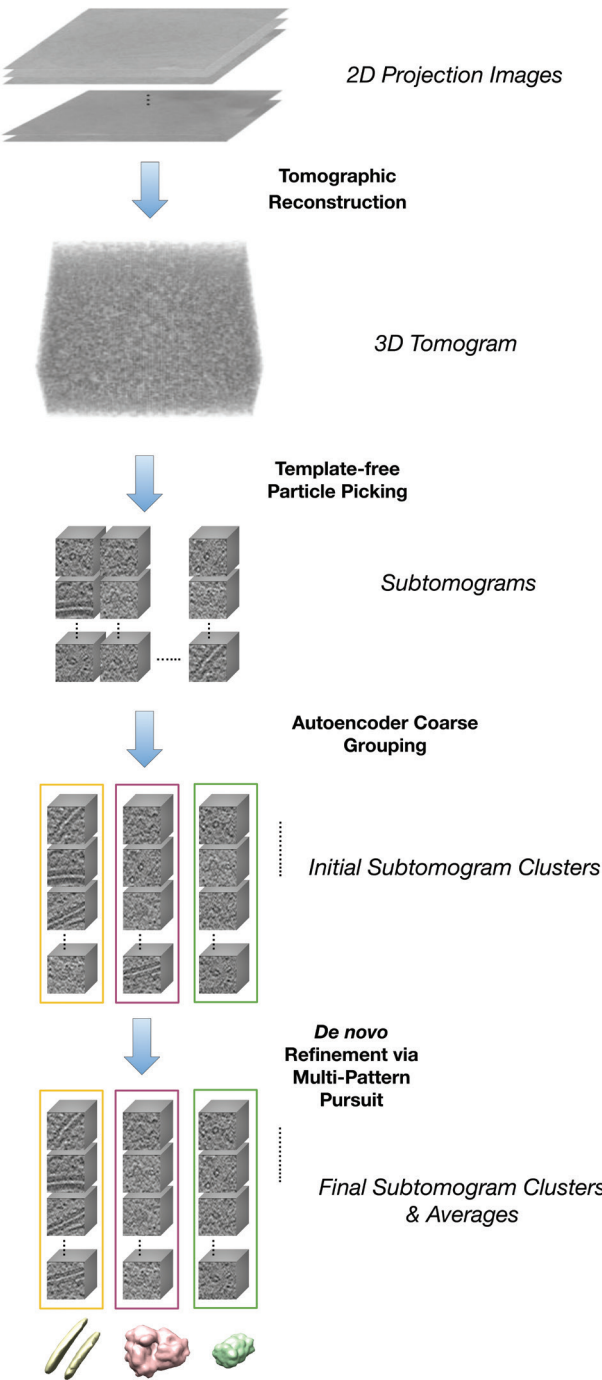


**Figure 1** Unsupervised structural pattern mining pipeline integrating the autoencoder and multi-pattern pursuit approach.



## Bacterial cell biology

Cryo-ET is capable of discovering detailed structure of bacterial cells in their native environment. Bacteria are viewed as structurally complex assemblies of macromolecular machines rather than undifferentiated bags of enzymes. This organization includes highly ordered arrays of chemosensory components (27, 28). Cryo-ET further enables the characterization of microcompartments for optimizing metabolism and storing nutrients (29–33). A visual inspection of more than 15,000 tomograms of intact frozen-hydrated cells belonging to 88 different bacterial species and several uncharacterized features in these tomograms has been reported (34). This has greatly improved our understanding of the complexity of bacterial cells. The advent of cryogenic focused ion beam (FIB) milling has extended the domain of Cryo-ET to include regions even deep within thick eukaryotic cells.

## Medical diagnosis

Since 2014, there has been a growing interest in the research community to establish Cryo-ET as a medical diagnostic tool to help resolve molecular differences between healthy and diseased states. Cryo-ET was applied to human clinical samples to elucidate human ciliary structural defects in patients with primary ciliary dyskinesia, where the conventional diagnosing tool EM failed 30% of the time (35). Later, Wang et al. (36) demonstrated the effectiveness of using Cryo-ET as a non-invasive tool to identify ovarian cancer patients by imaging their platelets. They built a simple model using the number of mitochondria and length of microtubules in Cryo-ET images and correctly predicted 20 out of 23 cases. Other studies have identified cellular structural changes in disease states such as Leigh syndrome (37), Huntington's disease (38), and virus infection (39).

---

## CONCLUSION

Cryo-ET led to a revolution in in-situ structural biology. However, due to the low SNR and structural complexity, it also poses challenges to the subsequent computational analysis. Template-based methods have enabled the systematic detection of known structures. To reduce the computational cost, a supervised deep learning-based approach was proposed to classify and segment cellular components. However, the success of such a supervised approach depends heavily on the availability of a large amount of properly labeled training data. The template-free approach has made it possible to automatically recover representative structures and the discovery of even unknown structures. Although the template-free approach has opened up promising new possibilities, the current accuracy and efficiency still has a large room for improvement. With an increasing amount of data being collected and an increasing amount of robust computational methods being developed, Cryo-ET has a large potential to advance structural biology and medical diagnosis progressively.

**Acknowledgement:** This work was supported in part by U.S. National Institutes of Health (NIH) grant P41 GM103712. XZ was supported by a fellowship from Carnegie Mellon University's Center for Machine Learning and Health. XG acknowledges the support by the King Abdullah University of Science and Technology (KAUST) Office of Sponsored Research (OSR) under Award No. BAS/1/1624, FCC/1/1976-18, FCC/1/1976-23, FCC/1/1976-25, and FCC/1/1976-26.

**Conflict of Interest:** The authors declare no potential conflicts of interest with respect to research, authorship, and/or publication of this chapter.

**Copyright and Permission Statement:** To the best of our knowledge, the materials included in this chapter do not violate copyright laws. All original sources have been appropriately acknowledged and/or referenced. Where relevant, appropriate permissions have been obtained from the original copyright holder(s)

## REFERENCES

1. Koning RI, Koster AJ, Sharp TH. Advances in cryo-electron tomography for biology and medicine. *Ann Anat.* 2018;217:82–96. <http://dx.doi.org/10.1016/j.aanat.2018.02.004>
2. Chang YW, Chen S, Tocheva EI, Treuner-Lange A, Löbach S, Søgaard-Andersen L, et al. Correlated cryogenic photoactivated localization microscopy and cryo-electron tomography. *Nat Methods.* 2014;11(7):737. <http://dx.doi.org/10.1038/nmeth.2961>
3. Xu M, Singla J, Tocheva EI, Chang YW, Stevens RC, Jensen GJ, et al. De Novo structural pattern mining in cellular electron cryotomograms. *Structure.* 2019;27(4):679–91.e14. Available from: <http://www.sciencedirect.com/science/article/pii/S096921261930005X>
4. Nickell S, Förster F, Linaroudis A, Del Net W, Beck F, Hegerl R, et al. TOM software toolbox: Acquisition and analysis for electron tomography. *J Struct Biol.* 2005;149(3):227–34. <http://dx.doi.org/10.1016/j.jsb.2004.10.006>
5. Förster F, Han BG, Beck M. Visual proteomics. *Methods Enzymol.* 2010;483:215–43. [http://dx.doi.org/10.1016/S0076-6879\(10\)83011-3](http://dx.doi.org/10.1016/S0076-6879(10)83011-3)
6. Beck M, Malmström JA, Lange V, Schmidt A, Deutsch EW, Aebersold R. Visual proteomics of the human pathogen *Leptospira interrogans*. *Nat Methods.* 2009;6(11):817. <http://dx.doi.org/10.1038/nmeth.1390>
7. Wang K, Zeng X, Liang X, Huo Z, Xing E, Xu M. Image-derived generative modeling of pseudo-macromolecular structures – Towards the statistical assessment of Electron CryoTomography template matching. In: *British Machine Vision Conference 2018, BMVC 2018, Northumbria University, Newcastle, UK, September 3–6, 2018*. p. 130. Available from: <http://bmvc2018.org/contents/papers/0532.pdf>
8. Chen M, Dai W, Sun SY, Jonasch D, He CY, Schmid MF, et al. Convolutional neural networks for automated annotation of cellular cryo-electron tomograms. *Nat Methods.* 2017;14(10):983. <http://dx.doi.org/10.1038/nmeth.4405>
9. Moebel E, Martinez A, Larivière D, Ortiz J, Baumeister W, Kervrann C. 3D ConvNet improves macromolecule localization in 3D cellular cryo-electron tomograms. 2018. <https://hal.inria.fr/hal-01966819/document>
10. Liu C, Zeng X, Lin R, Liang X, Freyberg Z, Xing E, et al. Deep learning based supervised semantic segmentation of electron cryo-subtomograms. In: *2018 25th IEEE International Conference on Image Processing (ICIP)*. IEEE; 2018. p. 1578–82.
11. Xu M, Chai X, Muthakana H, Liang X, Yang G, Zeev-Ben-Mordehai T, et al. Deep learning-based subdivision approach for large scale macromolecules structure recovery from electron cryo tomograms. *Bioinformatics.* 2017;33(14):i13–i22. <http://dx.doi.org/10.1093/bioinformatics/btx230>

12. Che C, Lin R, Zeng X, Elmaaroufi K, Galeotti J, Xu M. Improved deep learning-based macromolecules structure classification from electron cryo-tomograms. *Mach Vision Appl.* 2018;29(8):1227–36. <http://dx.doi.org/10.1007/s00138-018-0949-4>
13. Guo J, Zhou B, Zeng X, Freyberg Z, Xu M. Model compression for faster structural separation of macromolecules captured by cellular electron cryo-tomography. In: *International Conference Image Analysis and Recognition*. Springer; 2018. p. 144–52.
14. Han S, Mao H, Dally WJ. Deep compression: Compressing deep neural networks with pruning, trained quantization and huffman coding. *arXiv preprint arXiv:151000149*. 2015.
15. Meng W, Gu Z, Zhang M, Wu Z. Two-bit networks for deep learning on resource-constrained embedded devices. *arXiv preprint arXiv:170100485*. 2017.
16. Lin R, Zeng X, Kitani K, Xu M. Adversarial domain adaptation for cross data source macromolecule *in situ* structural classification in cellular electron cryo-tomograms. *Bioinformatics.* 2019;35(14):i260–8. <http://dx.doi.org/10.1093/bioinformatics/btz364>
17. Patel VM, Gopalan R, Li R, Chellappa R. Visual domain adaptation: A survey of recent advances. *IEEE Sig Process Mag.* 2015;32(3):53–69. <http://dx.doi.org/10.1109/MSP.2014.2347059>
18. Ganin Y, Ustinova E, Ajakan H, Germain P, Larochelle H, Laviolette F, et al. Domain-adversarial training of neural networks. *J Mach Learn Res.* 2016;17(1):2096–30.
19. Liu C, Zeng X, Wang K, Guo Q, Xu M. Multi-task learning for macromolecule classification, segmentation and coarse structural recovery in cryo-tomography. In: *British Machine Vision Conference 2018, BMVC 2018, Northumbria University, Newcastle, UK, September 3–6, 2018*. p. 271. Available from: <http://bmvc2018.org/contents/papers/1007.pdf>
20. Xu M, Beck M, Alber F. Template-free detection of macromolecular complexes in cryo electron tomograms. *Bioinformatics.* 2011;27(13):i69–76. <http://dx.doi.org/10.1093/bioinformatics/btr207>
21. Zhou B, Guo Q, Wang K, Zeng X, Gao X, Xu M. Feature decomposition based saliency detection in electron cryo-tomograms. In: *2018 IEEE International Conference on Bioinformatics and Biomedicine (BIBM)*. IEEE; 2018. p. 2467–73.
22. Zhao Y, Zeng X, Guo Q, Xu M. An integration of fast alignment and maximum-likelihood methods for electron subtomogram averaging and classification. *Bioinformatics.* 2018;34(13):i227–36. <http://dx.doi.org/10.1093/bioinformatics/bty267>
23. Bharat TA, Scheres SH. Resolving macromolecular structures from electron cryo-tomography data using subtomogram averaging in RELION. *Nat Protocols.* 2016;11(11):2054. <http://dx.doi.org/10.1038/nprot.2016.124>
24. Scheres SH, Melero R, Valle M, Carazo JM. Averaging of electron subtomograms and random conical tilt reconstructions through likelihood optimization. *Structure.* 2009;17(12):1563–72. <http://dx.doi.org/10.1016/j.str.2009.10.009>
25. Zeng X, Leung MR, Zeev-Ben-Mordehai T, Xu M. A convolutional autoencoder approach for mining features in cellular electron cryo-tomograms and weakly supervised coarse segmentation. *J Struct Biol.* 2018;202(2):150–60. <http://dx.doi.org/10.1016/j.jsb.2017.12.015>
26. Doerr A. Template-free visual proteomics. *Nature Methods.* 2019;16: 285
27. Briegel A, Li X, Bilwes AM, Hughes KT, Jensen GJ, Crane BR. Bacterial chemoreceptor arrays are hexagonally packed trimers of receptor dimers networked by rings of kinase and coupling proteins. *Proc Natl Acad Sci.* 2012;109(10):3766–3771. <http://dx.doi.org/10.1073/pnas.1115719109>
28. Liu J, Hu B, Morado DR, Jani S, Manson MD, Margolin W. Molecular architecture of chemoreceptor arrays revealed by cryoelectron tomography of *Escherichia coli* minicells. *Proc Natl Acad Sci.* 2012;109(23):E1481–8. <http://dx.doi.org/10.1073/pnas.1200781109>
29. Beeby M, Cho M, Stubbe J, Jensen GJ. Growth and localization of polyhydroxybutyrate granules in *Ralstonia eutropha*. *J Bacteriol.* 2012;194(5):1092–9. <http://dx.doi.org/10.1128/JB.06125-11>
30. Comolli LR, Kundmann M, Downing KH. Characterization of intact subcellular bodies in whole bacteria by cryo-electron tomography and spectroscopic imaging. *J Microscopy.* 2006;223(1):40–52. <http://dx.doi.org/10.1111/j.1365-2818.2006.01597.x>
31. Iancu CV, Ding HJ, Morris DM, Dias DP, Gonzales AD, Martino A, et al. The structure of isolated *Synechococcus* strain WH8102 carboxysomes as revealed by electron cryotomography. *J Mol Biol.* 2007;372(3):764–73. <http://dx.doi.org/10.1016/j.jmb.2007.06.059>

32. Pšenčík J, Collins AM, Liljeroos L, Torkkeli M, Laurinmäki P, Ansink HM, et al. Structure of chlorosomes from the green filamentous bacterium *Chloroflexus aurantiacus*. *J Bacteriol.* 2009;191(21):6701–8. <http://dx.doi.org/10.1128/JB.00690-09>
33. Schmid MF, Paredes AM, Khant HA, Soyer F, Aldrich HC, Chiu W, et al. Structure of *Halothiobacillus* eapolitanus carboxysomes by cryo-electron tomography. *J Mol Biol.* 2006;364(3):526–35. <http://dx.doi.org/10.1016/j.jmb.2006.09.024>
34. Dobro MJ, Oikonomou CM, Piper A, Cohen J, Guo K, Jensen T, et al. Uncharacterized bacterial structures revealed by electron cryotomography. *J Bacteriol.* 2017;199(17):e00100–17. <http://dx.doi.org/10.1128/JB.00100-17>
35. Lin J, Yin W, Smith MC, Song K, Leigh MW, Zariwala MA, et al. Cryo-electron tomography reveals ciliary defects underlying human RSPH1 primary ciliary dyskinesia. *Nat Commun.* 2014;5:5727. <http://dx.doi.org/10.1038/ncomms6727>
36. Wang R, Stone RL, Kaelber JT, Rochat RH, Nick AM, Vijayan KV, et al. Electron cryotomography reveals ultrastructure alterations in platelets from patients with ovarian cancer. *Proc Natl Acad Sci.* 2015;112(46):14266–71. <http://dx.doi.org/10.1073/pnas.1518628112>
37. Siegmund SE, Grassucci R, Carter SD, Barca E, Farino ZJ, Juanola-Falgarona M, et al. Three dimensional analysis of mitochondrial crista ultrastructure in a patient with leigh syndrome by in situ cryo-electron tomography. *iScience.* 2018;6:83–91. <http://dx.doi.org/10.1016/j.isci.2018.07.014>
38. Bäuerlein F, Mishra A, Dudanova I, Hipp M, Klein R, Hartl F, et al. Structural characterization of mutant huntingtin inclusion bodies by cryo-electron tomography. *Microsc Microanal.* 2016;22(S3):80–1. <http://dx.doi.org/10.1017/S1431927616001252>
39. Cao S, Maldonado JO, Grigsby IF, Mansky LM, Zhang W. Analysis of human T-cell leukemia virus type 1 particles by using cryo-electron tomography. *J Virol.* 2015;89(4):2430–5. <http://dx.doi.org/10.1128/JVI.02358-14>